

Generation and Characterization of Cytochrome P450 2J3/10 CRISPR/Cas9 Knockout Rat Model

Jian Lu, Ang Chen, Xinrun Ma, Xuyang Shang, Yuanjin Zhang, Yuanqing Guo,
Mingyao Liu, and Xin Wang

*Changning Maternity and Infant Health Hospital (J.L., Y.Z., Y.G., X.W.), and
Shanghai Key Laboratory of Regulatory Biology, Institute of Biomedical Sciences and
School of Life Sciences (J.L., A.C., X.M., X.S., Y.Z., M.L., X.W.), East China Normal
University, Shanghai, People's Republic of China*

Running title: CRISPR knockout rat CYP2J3/10 model

Address correspondence to:

Dr. Xin Wang,

Changning Maternity and Infant Health Hospital, School of Life Sciences, East China

Normal University, Shanghai 200241, China.

Tel: +86-21-2420 6564

Fax: +86-21-5434 4922

E-mail address: usxinwang@gmail.com, xwang@bio.ecnu.edu.cn

Number of text pages: 32

Number of tables: 3

Number of figures: 6

Number of references: 38

Number of words in the Abstract: 228

Number of words in the Introduction: 619

Number of words in the Discussion: 1295

Abbreviations

CYP2J2, cytochrome P450 2J2; AA, arachidonic acid; EETs, epoxyeicosatrienoic acids; WT, wild-type; SD, Sprague-Dawley; G6P, glucose 6-phosphate; G6PDH, glucose 6-phosphate dehydrogenase; NADP, β -nicotinamide adenine dinucleotide

phosphate hydrate; MRM, multiple reactions monitoring; KO, knockout; RLM, rat liver microsomes; $t_{1/2}$, half-life; MRT, mean retention time; ALB, albumin; GLB, globulin; TP, total proteins; AP, alkaline phosphatase; AST, aspartate amino transferase; ALT, alanine amino transferase; D-BIL, direct bilirubin; ID-BIL, indirect bilirubin; T-BIL, total bilirubin; TRIG, triglycerides; LDL-CHOL, low-density lipoproteins-cholesterol; HDL-CHOL, high-density lipoproteins-cholesterol; T-CHOL, total cholesterol; CK, creatine kinase.

Abstract

Cytochrome P450 2J2 (CYP2J2) enzyme attracts more attention because it not only metabolizes clinical drugs, but also mediates the biotransformation of important endogenous substances and the regulation of physiological function. Although CYP2J2 is very important, few animal models are available to study its function *in vivo*. In particular, *CYP2J* gene knockout (KO) rat model for drug metabolism and pharmacokinetics is not available. In this report, the CRISPR/Cas9 technology was used to delete rat *CYP2J3/10*, the orthologous genes of *CYP2J2* in humans. The *CYP2J3/10* KO rats were viable and fertile and showed no any off-target effect. Compared with wild-type (WT) rats, the mRNA and protein expression of *CYP2J3/10* in liver, small intestine and heart of KO rats were completely absent. At the same time, *CYP2J4* mRNA expression and protein expression were significantly decreased in these tissues. Further *in vitro* and *in vivo* metabolic studies of astemizole, a typical substrate of CYP2J, indicated that CYP2J was functionally inactive in KO rats. The heart function indexes of WT and KO rats were also measured and compared. The myocardial enzymes including creatine kinase-muscle brain type (CK-MB), creatine kinase (CK) and CK-MB/CK ratio of KO rats increased by nearly 140%, 80%, and 60%, respectively. In conclusion, this study successfully developed a new *CYP2J3/10* KO rat model, which is a useful tool to study the function of CYP2J in drug metabolism and cardiovascular disease.

Key words: CYP2J; CRISPR/Cas9; Cardiovascular disease; Drug metabolism; Rat model

Significance Statement

Human CYP2J2 is not only involved in clinical drug metabolism, but also in the biotransformation of important endogenous substances. Therefore, it is very important to construct new animal models to study its function *in vivo*. This study successfully developed a new CYP2J knockout rat model by using the CRISPR/Cas9 technology. This rat model provides a useful tool to study the role of CYP2J in drug metabolism and diseases.

Introduction

Human cytochrome P450 2J2 (CYP2J2) enzyme is involved in the metabolism of about 3% clinical drugs, which mainly include some antihistamines, such as astemizole, ebastine, and terfenadine (Xu et al., 2013; Zanger and Schwab, 2013). CYP2J2 is not only mainly expressed in human heart and liver (Askari et al., 2013; Lu et al., 2018), but also in tumors (Chen et al., 2011). In addition to drug metabolism, CYP2J2 is also involved in metabolism of endogenous substances such as arachidonic acid (AA), linoleic acid, eicosapentaenoic acid, docosahexaenoic acid and vitamin D3 (Xu et al., 2013). AA is a polyunsaturated fatty acid with important physiological functions (Xu et al., 2013; Chen et al., 2011). Epoxyeicosatrienoic acids (EETs) are derived from CYP2J2-mediated AA metabolism (Chen et al., 2011). CYP2J2 can protect cardiac function in myocardial infarction-induced heart failure by increasing the concentration of circulating EETs and promoting angiogenesis through Jagged1/Notch1 signaling pathway (Zhao et al., 2018). In addition, CYP2J2 inhibitor can significantly reduce the proliferation, migration and promote apoptosis of tumor cells by inhibiting the biosynthesis of EETs (Lu et al., 2018; Chen et al., 2011). Therefore, CYP2J2 plays a crucial role in drug metabolism and diseases.

In 2013, the *Cyp2j* locus was deleted through fusion BAC-mediated recombination, and the role of *Cyp2j* in hypoxic pulmonary vascular response was explored in this knockout mouse model (Zhou et al., 2013). In 2015, the role of CYP2J in pulmonary vascular remodeling and hypertension in mice was also discussed (Beloiartsev et al.,

2015). The anti-inflammatory effect of CYP2J in macrophage is also revealed by a *CYP2J4* knockout (KO) rat model (Behmoaras et al., 2015). However, *CYP2J3/10* KO animal model is not available. *CYP2J* KO rat model is important for pharmacological research, especially for drug metabolism and pharmacokinetic (DMPK) studies. Rats possess larger body size and have more body fluids, which are conducive to DMPK studies (Lu et al., 2017). Moreover, it is reported that the rat model shows advantages over mouse model for the study of cardiovascular diseases (Iannaccone and Jacob, 2009; Zhao et al., 2018). As the third generation of artificial nuclease technology, the clustered regularly interspaced short palindromic repeat (CRISPR)/CRISPR-associated 9 (Cas9) system has become the most important gene editing tool (Shao et al., 2014; Wang et al., 2016). CRISPR/Cas9 has made an important breakthrough in the construction of transgenic animal models and targeted gene therapy (Shao et al., 2014). CRISPR/Cas9, as a new gene editing technology, has the characteristics and advantages of accurate target, simple operation, simultaneous knockout of multiple target genes, and no species restriction (Shao et al., 2014; Li et al., 2019). In recent years, scientists have made important progress in the construction of rat DMPK models by using the CRISPR/Cas9 technology (Li et al., 2019). For example, in terms of rat DMPK models, we have successfully constructed *Cyp2e1* (Wang et al., 2016), *Cyp3a1/2* (Lu et al., 2017), *Mdr1a/b* (Liang et al., 2019), and *Slco1b2* (Ma et al., 2020) gene KO rats by using the CRISPR/Cas9 system. These rat DMPK models are further used in the study of drug metabolism and transport, pharmacodynamic, toxicity, and disease-related molecular mechanism, strengthening the relationship between DMPK and

pharmacology/toxicology, and promoting the new development of drug metabolism in innovative animal models (Qin et al., 2017; Ma et al., 2019).

In this report, the CRISPR/Cas9 technology is applied to the construction of the innovative rat *CYP2J3/10* KO rat model, which can efficiently get the KO rats, significantly reduce the modeling cost, and shorten the modeling time. Further pharmacokinetic studies of astemizole, a typical substrate of CYP2J, confirmed the KO rats lost the CYP2J metabolic function *in vivo*. This rat model provides a useful tool to study the role of CYP2J in drug metabolism and diseases.

Materials and Methods

Materials and chemicals

Oligos (60 bp, containing *CYP2J3* or *CYP2J10* knockout target-sites) and all primers for PCR were ordered from Biosune Biotechnology Co. LTD (Shanghai, China). Ethidium bromide was obtained from TianGen biotechnology Company (Beijing, China). Trizol, TA cloning kit, Prime Script RT Reagent Kit, SYBR Premix Ex Taq and *in vitro* Transcription T7 Kit were bought from Takara (Dalian, China). The mMessage mMachine SP6 kit was bought from Thermo Scientific (Massachusetts, USA). Enzyme-linked immunosorbent assay (ELISA) kits for the detection of CYP2J3, CYP2J4 and CYP2J10 protein were purchased from Jiangsu Meimian industrial Co., Ltd (Jiangsu, China). Astemizole was bought from MeilunBio (Dalian, China), and *O*-desmethyl astemizole was purchased from

Toronto Research Chemicals (Toronto, Canada). Glucose 6-phosphate (G6P), glucose 6-phosphate dehydrogenase (G6PDH), β -nicotinamide adenine dinucleotide phosphate hydrate (NADP) and tribromoethanol were bought from sigma (St. Louis, USA). Tris base was purchased from Amresco (OH, USA). The internal standard (mebendazole) for LC-MS/MS was purchased from Aladdin (Shanghai, China).

Animals

All wild-type (WT) male and female Sprague-Dawley (SD) rats used for gene targeting were purchased from the National Rodent Laboratory Animal Resources. All WT rats used in this research were littermate control of KO rats. Both WT and KO rats were kept under a specific pathogen-free facility with access to sterile water and rodent chow cubes, with 12 h light-dark cycles. The research was conducted in accordance with the Declaration of Helsinki and/or with the Guide for the Care and Use of Laboratory Animals as adopted and promulgated by the United States National Institutes of Health. All the animal experiment protocols in this study were approved by the Ethics Committee on Animal Experimentation of East China Normal University (Shanghai, China).

Generation of CYP2J3/10 knockout rat model

The *CYP2J3/10* KO rat model was generated through CRISPR/Cas9 system and the gene targeting method was reported in our previous studies with some modifications (Wang et al., 2016; Lu et al., 2017). The sequence fragments of *CYP2J3* and *CYP2J10*

were submitted to a CRISPR Design Tool (<http://tools.genome-engineering.org>) to get target sites (an 18 bp DNA sequence with a PAM site (5'-NGG-3') in the 3' end). Oligo DNA sequence (60 bp) containing 18 bp target sequence and T7 promoter was synthesized *in vitro*. By overlapping PCR, oligos (60 bp) were linked to the pGS3-T7-gRNA vector for sgRNA transcription. sgRNAs were produced by using T7 Transcription Kit and purified with phenol/chloroform extraction method. Expression vectors for Cas9 were digested with Not I and then extracted by phenol/chloroform extraction methods. Cas9 mRNA was transcribed by using the mMessage mMachine SP6 kit and recovered by Lithium chloride precipitation. The final concentrations of *CYP2J3* sgRNA, *CYP2J10* sgRNA and Cas9 mRNA for micro-injection were 30 ng/μL, 30 ng/μL and 50 ng/μL, respectively. Cas9 online designer (<http://cas9.wicp.net/>) was used to evaluate potential off-target sites for the two sgRNA and off-target sites with a score ≥ 0.25 were selected for validation, using T7E1 assay. All primer pairs used in the generation of CYP2J KO rat model were listed in Table 1, including primer pairs for genotyping and off-target evaluation.

Real-time PCR

Male SD rats (about 8 weeks) were sacrificed with carbon dioxide asphyxiation. Tissues were isolated as soon as possible and stored at -80 °C for further processing. All tissues were adequately grinded under the atmosphere of liquid nitrogen and then transferred into tubes. Trizol was added into tubes for the lysis of tissues and total mRNA was extracted according to the instruction of the manufacturer. Total RNA was

then reverse-transcribed into cDNA using the Takara RR036A RT kit. Real-time PCR was performed by using a Stratagene Mx3005P with SYBR Premix Ex Taq. All primer pairs used for real-time PCR were listed in Table 1. In order to detect the mRNA expression of *CYP2J3*, the primer pair (*CYP2J3*-Q-PCR-F/R) was designed on the downstream sequence of the sgRNA target site, and exon 1 to exon 3 of *CYP2J3* gene was amplified. In order to detect the mRNA expression of *CYP2J10*, the primer pair (*CYP2J10*-Q-PCR-F/R) was designed on the downstream sequence of the sgRNA target site, and exon 1 to exon 2 of *CYP2J10* gene was amplified. The PCR products for *CYP2J3* and *CYP2J10* mRNA detection were 268 bp and 235 bp, respectively.

Enzyme-linked immunosorbent assay

ELISA was conducted to detect the protein expression of CYP2J isoforms in rats. Male SD rats (about 8 weeks) were sacrificed with carbon dioxide asphyxiation. Tissues (liver, small intestine and heart) were isolated as soon as possible and stored at -80 °C for further processing. Phosphate buffer solution (PBS, 1 mL) was added into tissues (100 mg) and then tissues were homogenized under the temperature of 4 °C. The homogenate was then centrifuged at 4 °C, 3,000 g for 20 min. The supernatant was collected for further use. The method of ELISA detection is according to the product instructions with some modification. Standard samples and test samples (tissues supernatant) were added into 96-well plate respectively, and the enzyme-labeled reagent (100 µL) was added into each well. Then, the plate was incubated at 37 °C for 60 min, and then washed with washing buffer for 5 times. Developer A (50 µL) and

developer B (50 μ L) were added into each well, and then the plate was shaken gently to mix, followed by the incubation at 37 °C for 15 min in the dark. After incubation, the reaction was stopped by adding the stop solution (50 μ L). Finally, the absorbance (OD value) of each well was measured at 450 nm wavelength after setting the zero point by using the blank control well.

Metabolic capacity of CYP2J in WT and KO rats *in vitro*

Methods for the preparation of rat liver microsomes (RLM, from 8 weeks, male rats) were modified from our previous studies (Wang et al., 2010; Wang and Yeung, 2011). Astemizole was used as the probe substrate and the reaction of astemizole *O*-demethylation was monitored for the evaluation of CYP2J metabolic activity *in vitro* (Lu et al., 2018). The incubation mixture contained an NADPH regenerating system (5 mM G6P, 0.4 U/mL G6PDH and 1 mM NADP), astemizole (0.2 μ M to 10 μ M) and 0.1 mg/mL of RLM in 0.05 M Tris-HCl buffer (pH 7.4). The incubation was stopped by precooled acetonitrile after 20 min incubation. The internal standard (mebendazole) was added, and the supernatant of the incubation mixture was then transferred to the autosampler vial after a protein precipitation process for LC-MS/MS analysis. According to the standard Michaelis-Menten equation, K_m and V_{max} were analyzed by GraphPad Prism 6.0 (GraphPad Software Inc., San Diego, CA) and the V_{max}/K_m ratio was defined as CL_{int} .

Pharmacokinetic analysis of astemizole in WT and KO Rats

Astemizole (20 mg/kg) was administered through gavage for all WT and KO rats (8 weeks, male), and blood samples (300 μ L) were collected into heparinized centrifuge tubes at 5, 15, 30, 45, 60, 120, 180, 240, 300 and 420 min through caudal vein with capillary tubes. Blood samples were centrifuged at 5,500 g for 15 min at 4 $^{\circ}$ C, and the plasma was transferred into new tubes and frozen at -80 $^{\circ}$ C for further detection. Protein precipitation was applied for the pretreatment of plasma samples. Acetonitrile (300 μ L) and internal standard (mebendazole, 10 μ L) were added to 100 μ L plasma orderly, followed by the centrifugation at 4 $^{\circ}$ C, 14,000 g for 15 min. The supernatant (70 μ L) was transferred into the autosampler vial for LC-MS/MS detection.

Methods for LC-MS/MS analysis

For the LC-MS/MS detection, a 1290 HPLC-6460 triple quadrupole mass spectrometer coupled with ESI ion source (Agilent Technologies, USA) was employed. For the detection of astemizole and its metabolite *O*-demethylastemizole in both RLM incubation mixture and plasma, the mobile phase consisted of water (A) with 0.1% formic acid and acetonitrile (B) with 0.1% formic acid was applied. Astemizole and *O*-demethylastemizole were eluted by gradient with a flow rate of 0.3 mL/min as follows: 0-1 min, 20% acetonitrile; 1-3.5 min, 20%-80% acetonitrile; 3.5-4.5 min, 80% acetonitrile; 4.5-5 min, 80%-20% acetonitrile; 5-8 min, 20% acetonitrile. The detection of the ions was performed in a positive multiple reaction monitoring (MRM) mode,

monitoring the transition of m/z 459.2 to 218.2 for astemizole, m/z 445.2 to 121.2 for *O*-demethylastemizole and m/z 296.1 to 264.1 for internal standard mebendazole.

Clinical chemistry analysis of WT and KO rats

Blood from eight weeks old male rats was collected through caudal vein, and the serum was prepared by the following steps below: standing at 4 °C for 30 min, centrifugation at 4 °C, 1,500 g for 15 min. Then the serum supernatant was transferred into a new tube and stored at -80 °C for further use. Serum samples were sent to ADICON Clinical Laboratories (Shanghai, China) for the detection of biochemical criterions, including albumin (ALB), globulin (GLB), ALB/GLB, total proteins (TP), alkaline phosphatase (AP), aspartate amino transferase (AST), alanine amino transferase (ALT), AST/ALT, direct bilirubin (D-BIL), ID-BIL (indirect bilirubin), total bilirubin (T-BIL), triglycerides (TRIG), low-density lipoproteins-cholesterol (LDL-CHOL), high-density lipoproteins-cholesterol (HDL-CHOL), total cholesterol (T-CHOL), HDL-CHOL/ LDL-CHOL, creatine kinase (CK), CK-MB and CK-MB/CK.

Statistical analysis

All data was presented as mean \pm standard deviation (SD). Statistical analysis between different groups was performed using two-tailed t-test and *p*-values less than 0.05 were considered to indicate statistical significance. The pharmacokinetic parameters of astemizole were calculated by WinNonlin professional version 5.2.1 (Pharsight Mountain View, CA) based on the non-compartmental method.

Results

Generation of CYP2J3/10 knockout rat model

According to the results from “CRISPR DESIGN”, 5'-CCCCAAGAAGTACCCGCC-3' (followed with AGG) and 5'-GGTGTAACAGGGCGATTC-3' (followed with AGG) were selected as target sites for rat *CYP2J3* and *CYP2J10*, respectively. The quality of *CYP2J3* and *CYP2J10* sgRNA was good enough for injection, which was determined through agarose gel electrophoresis (Fig. 1A-B). After co-injection of *CYP2J3* sgRNA, *CYP2J10* sgRNA and Cas9 mRNA into one-cell fertilized eggs of SD rats, 5 progenies were born. For identification of gene modifications in F₀ generation progeny, sequence flanking target sites were amplified through PCR and the products were digested with T7EI. For *CYP2J3*, PCR products of 3 progenies (F₀-2#, 3#, 4#) were detected with T7EI cleavage, which indicated the potential of gene modification around the target sites (Fig. 1C). The PCR product was inserted into the T vector, and the sequencing of T vector further revealed that all three progenies contained the same 10 bp deletion at the target site (Fig. 1D). For *CYP2J10*, amplification of sequence flanking the target site was not succeeded for F₀-3#, 5#, until the product size was enlarged to more than 3 kb. This demonstrated a large-scale deletion possibility and direct sequencing of these products showed an 1199 bp deletion around the target site for both F₀-3# and F₀-5# (Fig. 1C-D). Thus, F₀-3# was selected for the breeding of homozygous, KO rats, and finally F₂ progenies with 10 bp deletion for *CYP2J3* and 1199 bp deletion for *CYP2J10* were gained.

Off-target analysis

Off-target effects of CRISPR/Cas9 system, targeting *CYP2J3* and *CYP2J10*, were searched on a genome wide sgRNA off-target searching tool (<http://cas9.wicp.net/>) and then evaluated by T7EI cleavage assay. Off-target sites with a relatively high off-target score (≥ 0.25) were selected for T7EI treatment (Table 2). Agarose gel electrophoresis results showed no off-target effect in all high potential off-target sites (Fig. 2).

Expression of CYP2J in tissues of WT and KO rats

The mRNA expression of *CYP2J3*, *CYP2J4* and *CYP2J10* in rat liver, small intestine and heart was detected through specific primer pairs (Table 1). Agarose gel electrophoresis results verified that no mRNA expression of *CYP2J3*, *CYP2J4* and *CYP2J10* was detected in above tissues of KO rats, while it was highly expressed in WT control of these corresponding tissues (Fig. 3A).

The protein levels of *CYP2J3*, *CYP2J4* and *CYP2J10* in rat liver, small intestine and heart were detected by ELISA. *CYP2J3* was not detected in the liver of KO rats, while *CYP2J4* and *CYP2J4* decreased by about 80% and 90% (Fig. 3B), respectively. *CYP2J3* and *CYP2J10* in the small intestine of KO rats were undetectable, while *CYP2J4* decreased by around 75% (Fig. 3B). In the heart of KO rats, *CYP2J3*, *CYP2J4* and *CYP2J10* decreased about 90%, 60%, and 90% (Fig. 3B), respectively.

Metabolic capacity of CYP2J in WT and KO rats *in vitro*

To assess the metabolic function of CYP2J in the KO rat *in vitro*, astemizole was chosen as a probe substrate to characterize the metabolic activity of CYP2J in rat liver microsomes (RLM). In the RLM of WT rats, the *O*-desmethylastemizole was formed

effectively, compared with that in RLM of KO rats (Fig. 4A-C). The apparent K_m values for the metabolism of astemizole in the RLM of WT and KO rats were 8.2 μM and 9.7 μM , respectively. The V_{max} of astemizole metabolism in KO rats was decreased to 40% of that in WT rats, and the Cl_{int} was also decreased to 35% of that in WT rats (Fig. 4B-C). All these results indicated that the CYP2J activity of KO rats was significantly decreased *in vitro*.

Metabolic capacity of CYP2J in WT and KO rats *in vivo*

To further assess the metabolic function of CYP2J in the KO rat *in vivo*, the pharmacokinetics behavior of astemizole was monitored and compared between WT and KO rats. After oral administration of astemizole, the metabolic rate of KO rats was much slower, and the AUC was 4.6 times higher than that of WT rats (Table 3, Fig. 4D, E). At the same time, the C_{max} of astemizole in KO rats was significantly increased, with 2.4 times of that in WT rats (Table 3). *CYP2J3/10* KO also prolonged the half-life ($t_{1/2}$, 3.4 times of that in WT rats) and mean retention time (MRT, 1.4 times of that in WT rats), and decreased the CL/F and V_d/F values (Table 3). Therefore, the pharmacokinetic results were consistent with the data of *in vitro* metabolic activity test, indicating that CYP2J lost its metabolic function in KO rats.

Clinical biochemical criterion analysis of WT and KO rats

In addition to drug metabolism, CYP2J2 is also a great contributor to the biotransformation of physiological substances and plays an important role in human health. The loss of *CYP2J* genes in rats may cause some physiological changes, and thus the clinical chemistry analysis was carried out. Compared with WT rats,

CYP2J3/10 KO in rats showed no significant difference of serum protein, alkaline phosphatase, transaminase, bilirubin, triglyceride, and cholesterol (Fig. 5A). Since *CYP2J2* is necessary for cardiac function, the biomarkers of myocardial function are also measured and compared. The results showed that the values of CK-MB, CK and CK-MB/CK of KO rats significantly increased by almost 140%, 80%, and 60%, respectively, indicating that KO rat cardiomyocytes had the potential of injury (Fig. 5B).

Compensatory expression of other CYP isoforms and nuclear receptors in *CYP2J* KO rats

The deficiency of *CYP2J3/10* may affect the expression of other CYP isoforms and nuclear receptors in rats. Thus mRNA expression of other main CYP isoforms and nuclear receptors in the liver, small intestine and heart were measured by real time-PCR. *Cyp1a2* mRNA expression in the WT liver decreased by about 50% of that in the KO rat liver, while the expression of *Cyp3a2* significantly increased by about 80% (Fig. 6A). No significant change was observed in the small intestinal expression of all tested CYP isoforms and nuclear receptors (Fig. 6B). In the heart tissue of KO rats, *Cyp1a2*, *Cyp2e1*, *Cyp3a1* and *Cyp3a2* were up-regulated by about 60%, 140%, 180% and 260%, respectively (Fig. 6C).

Discussion

CYP2J2 is the only isoenzyme of human *CYP2J* subfamily, while there are three *CYP2J* subtypes (*CYP2J3*, *CYP2J4* and *CYP2J10*) in rat genome. Compared with human *CYP2J2* cDNA, the homology of *CYP2J3*, *CYP2J4* and *CYP2J10* cDNA is 79%,

80%, and 78%, respectively (data from NCBI). Human *CYP2J2* is mainly expressed in the heart and liver, and the expression pattern of *CYP2J3* in rats is similar (Xu et al., 2013). *CYP2J10* is also expressed in rat aorta (Di Pascoli et al., 2015). However, *CYP2J4* shows a different expression pattern compared with human *CYP2J2* (Zhang et al., 1998; Xu et al., 2013). Additionally, *CYP2J3* shows similar metabolic preference to human *CYP2J2* on some endogenous substance, such as AA (Xu et al., 2013). Therefore, *CYP2J3* and *CYP2J10* were selected in this study to investigate the effect of *CYP2J* deficiency on the metabolic functions in rats.

In order to achieve effective target gene editing, we selected the target site at the first exon of *CYP2J3*, and finally obtained homozygotes with 10 bp deletion around the target site, which causes frame shift mutation of *CYP2J3*. For *CYP2J10* targeting, a preferential target was found and chosen at the second exon. However, the sgRNA targeting *CYP2J10* tends to induce the large-scale deletion on both sides of the target site, resulting in homozygous *CYP2J10* with 1199 bp deletion. The same phenomenon has been reported in previous studies, that is, even if only one sgRNA is introduced into the zygote, there may be a deletion extending more than thousands of bases (Kosicki et al., 2018). It is reported that CRISPR/Cas9 system can tolerate a 1~3 base pair mismatch in its target sequence (Shao et al., 2014). Therefore, the off-target effects in *CYP2J3/10* KO rat model were evaluated. Under the threshold value of 0.25, only 6 and 2 potential off-target sites were selected for *CYP2J3* and *CYP2J10* sgRNA, respectively, which indicated a low off-target possibility of the target sites used in this study. No off-target effect was observed among these 8 potential off-target sites by

T7E1 assay. Furthermore, the PCR products were sequenced directly to verify the results from T7E1 assay (data not shown).

Our results showed the mRNA expression of *CYP2J3/10* was completely absent in the liver, small intestine, and heart of KO rats. The protein level of CYP2J3 in the liver and small intestine of KO rats was undetectable, while it was detected in the heart of KO rats with a very low level (<10%, compared with that in the WT group). Since the protein level of *CYP2J3* was measured using ELISA, we speculate that the detected value in the heart of KO rats was the background value after the endogenous CYP2J3 is missing. Similarly, the protein level of CYP2J10 in the small intestine of KO rats was undetectable and the levels in the liver and heart of KO rats were also very low (<10%, compared with that in the WT group). In order to evaluate the compensation of *CYP2J4* after *CYP2J3/10* knockout, the mRNA and protein expression of *CYP2J4* in KO rats were measured. The mRNA expression of *CYP2J4* was also completely absent in the liver, small intestine, and heart of KO rats. However, the protein expression of *CYP2J4* in the liver, small intestine, and heart of KO rats decreased by 80%, 75%, and 60%, respectively. We speculate that *CYP2J4*, *CYP2J3* and *CYP2J10* share some regulatory regions and sequence, because they are orderly located on 5q33 of Chromosome 5 and close to each other. Therefore, the deletion of *CYP2J3* and *CYP2J10* sequence may interfere with the regulation region and sequence of *CYP2J4*, and eventually lead to the down regulation of *CYP2J4*. Our initial aim was to knock out *CYP2J3* and *CYP2J10*, but unexpectedly decreased the expression of *CYP2J4*. Such a model may be more conducive to study the function of CYP2J.

In order to further confirm the deficiency of metabolic function of CYP2J, its metabolic ability was evaluated both *in vitro* and *in vivo*. Although other CYP isoforms, such as CYP2D6 and CYP4F12, may be involved in the catalytic action of the conversion of astemizole to *O*-demethylated astemizole, CYP2J is still the primary drug metabolizing enzyme that mediates this reaction (Matsumoto and Yamazoe, 2001; Matsumoto et al., 2003; Xu et al., 2013). Therefore, astemizole is selected as the probe substrate of CYP2J metabolic capacity phenotype in rats (Matsumoto et al., 2003; Lu et al., 2018). The RLM incubation and pharmacokinetics of astemizole indicated that the metabolic function of CYP2J was decreased in KO rats. The residual metabolic activity of KO group may be related to other CYP isoforms in rats. Therefore, the *CYP2J3/10* KO rat model was generated successfully by using CRISPR/Cas9 technology. To our knowledge, it is the first time to obtain *CYP2J3/10* KO rats, which are a good tool to study CYP2J-mediated drug metabolism *in vivo*.

CYP2J is also involved in the metabolism of various endogenous substances and may play a role in physiological functions. Thus, the basic physiological status of KO rats was evaluated through clinical chemistry analysis. Compared with WT rats, *CYP2J3/10* deficiency had no effect on serum protein, alkaline phosphatase, transaminase, bilirubin, triglyceride and cholesterol. However, myocardial enzyme CK, CK-MB, and the ratio (CK-MB/CK) significantly increased by 140%, 80%, and 60%, respectively. Actually, the myocardial enzyme CK-MB is often used as a biomarker for the diagnosis of myocardial injury (Hueb et al., 2012; Al-Hadi and Fox, 2009), because it mainly exists in the heart muscle with relatively high concentration. In addition, the CK-MB index

(CK-MB/CK) is a specific parameter to evaluate the relative contribution of cardiomyocyte damage, compared with other non-specific myocardial cell injury (Saenger and Jaffe, 2007). In this study, *CYP2J3/10* deficiency increased serum CK-MB concentration and the ratio of CK-MB/CK. These results suggested that there may be myocardial injury in KO rats, which needs further study.

AA and EETs, as essential polyunsaturated fatty acids, have many biological functions, especially in human heart (Murray, 2016). CYP2J2 is a principal enzyme that promotes the biotransformation of AA to EETs in myocardial cells (Imig, 2012; He et al., 2017). In recent years, a series of studies have focused on the cardioprotection of AA-CYP2J2-EETs pathway (Ai et al., 2009; Imig, 2012; Ma et al., 2013; Fleming, 2014). In this study, the deletion of *CYP2J3/10* was used to simulate the loss of function mutation of *CYP2J2* in human body. The results revealed that *CYP2J3/10* deficiency had some effects on cardiac function. Therefore, *CYP2J3/10* is an important factor, not the only one, to maintain the EETs concentrations *in vivo*. Other CYPs, such as CYP2C and CYP3A, have also been reported to mediate the biotransformation of AA to EETs (Panigrahy et al., 2010; Mitra et al., 2011). Therefore, the compensatory effect of other CYPs in KO rats should be considered.

Last but not least, aging is a major risk factor for myocardial disease, which promotes changes in the structure and function of the heart, leading to deterioration in some patients with acute myocardial infarction (Boon et al., 2013; Roh et al., 2016). Therefore, we speculate that the effect of *CYP2J3/10* deficiency on cardiac function of rats may become more and more serious in the process of aging. Further research should

be carried out to make sure this issue.

In conclusion, this study successfully developed a new *CYP2J3/10* KO rat model, which provides a useful tool for the study of CYP2J in drug metabolism and diseases. *CYP2J3/10* deficiency not only significantly reduced the metabolism of astemizole, but also increased myocardial enzymes (CK and CK-MB) and their ratio (CK-MB/CK), which is a typical sign of myocardial injury. The present study provides a preliminary assessment of the role of CYP2J in drug metabolism and its potential impact on cardiac function.

Conflict of interest

The authors declare no conflicts of interest.

Author contributions

Participated in research design: Liu and Wang.

Conducted experiments: Lu, Chen, Ma, Shang, and Zhang.

Performed data analysis: Lu and Wang.

Wrote or contributed to the drafting of the manuscript: Lu, Guo, and Wang.

References

- Ai D, Pang W, Li N, Xu M, Jones PD, Yang J, Zhang Y, Chiamvimonvat N, Shyy JY, Hammock BD, and Zhu Y (2009) Soluble epoxide hydrolase plays an essential role in angiotensin II-induced cardiac hypertrophy. *Proc Natl Acad Sci U S A* **106**:564-569.
- Askari A, Thomson SJ, Edin ML, Zeldin DC, and Bishop-Bailey D (2013) Roles of the epoxygenase CYP2J2 in the endothelium. *Prostaglandins Other Lipid Mediat* **107**: 56–63.
- Behmoaras J, Diaz AG, Venda L, Ko JH, Srivastava P, Montoya A, Faull P, Webster Z, Moyon B, Pusey CD, Abraham DJ, Petretto E, Cook TH, and Aitman TJ (2015) Macrophage epoxygenase determines a profibrotic transcriptome signature. *J Immunol* **194**:4705-4716.
- Beloiartsev A, da Gloria Rodrigues-Machado M, Zhou GL, Tan TC, Zazzeron L, Tainsh RE, Leyton P, Jones RC, Scherrer-Crosbie M, and Zapol WM (2015) Pulmonary hypertension after prolonged hypoxic exposure in mice with a congenital deficiency of Cyp2j. *Am J Respir Cell Mol Biol* **52**:563-570.
- Boon RA, Iekushi K, Lechner S, Seeger T, Fischer A, Heydt S, Kaluza D, Treguer K, Carmona G, Bonauer A, Horrevoets AJ, Didier N, Girmatsion Z, Biliczki P, Ehrlich JR, Katus HA, Muller OJ, Potente M, Zeiher AM, Hermeking H, and Dimmeler S (2013) MicroRNA-34a regulates cardiac ageing and function. *Nature* **495**:107-110.

Chen C, Wei X, Rao X, Wu J, Yang S, Chen F, Ma D, Zhou J, Dackor RT, Zeldin DC, and Wang DW (2011) Cytochrome P450 2J2 is highly expressed in hematologic malignant diseases and promotes tumor cell growth. *J Pharmacol Exp Ther* **336**: 344–355.

Di Pascoli M, Turato C, Zampieri F, Verardo A, Pontisso P, Pesce P, Sacerdoti D, and Bolognesi M (2015) Changes in gene expression of cytochrome P-450 in liver, kidney and aorta of cirrhotic rats. *Prostaglandins Other Lipid Mediat* **120**:134-138.

Fleming I (2014) The pharmacology of the cytochrome P450 epoxygenase/soluble epoxide hydrolase axis in the vasculature and cardiovascular disease. *Pharmacol Rev* **66**:1106-1140.

He Z, Yang Y, Wen Z, Chen C, Xu X, Zhu Y, Wang Y, and Wang DW (2017) CYP2J2 metabolites, epoxyeicosatrienoic acids, attenuate Ang II-induced cardiac fibrotic response by targeting Galpha12/13. *J Lipid Res* **58**:1338-1353.

Hueb W, Gersh BJ, Rezende PC, Garzillo CL, Lima EG, Vieira RD, et al. (2012) Hypotheses, rationale, design, and methods for prognostic evaluation of cardiac biomarker elevation after percutaneous and surgical revascularization in the absence of manifest myocardial infarction. A comparative analysis of biomarkers and cardiac magnetic resonance. The MASS-V Trial. *BMC Cardiovasc Disord* **12**:65.

Iannaccone PM and Jacob HJ (2009) Rats! *Dis Model Mech* **2**:206-210.

Imig JD (2012) Epoxides and soluble epoxide hydrolase in cardiovascular physiology.

Physiol Rev **92**:101-130.

Kosicki M, Tomberg K, and Bradley A (2018) Repair of double-strand breaks induced by CRISPR-Cas9 leads to large deletions and complex rearrangements. *Nat Biotechnol* **36**:765-771.

Li Y, Meng Q, Yang M, Liu D, Hou X, Tang L, Wang X, Lyu Y, Chen X, Liu K, Yu A, Zuo Z, and Bi H (2019) Current Trends in Drug Metabolism and Pharmacokinetics. *Acta Pharm Sin B* **9**:1113-1144.

Liang C, Zhao J, Lu J, Zhang Y, Ma X, Shang X, Li Y, Ma X, Liu M, and Wang X (2019) Development and characterization of MDR1 (Mdr1a/b) CRISPR/Cas9 knockout rat model. *Drug Metab Dispos* **47**:71-79.

Lu J, Liu D, Zhou X, Chen A, Jiang Z, Ye X, Liu M, and Wang X (2018) Plant natural product plumbagin presents potent inhibitory effect on human cytochrome P450 2J2 enzyme. *Phytomedicine* **39**:137-145.

Lu J, Shao Y, Qin X, Liu D, Chen A, Li D, Liu M, and Wang X (2017) CRISPR knockout rat cytochrome P450 3A1/2 model for advancing drug metabolism and pharmacokinetics research. *Sci Rep* **7**:42922.

Ma B, Xiong X, Chen C, Li H, Xu X, Li X, Li R, Chen G, Dackor RT, Zeldin DC, and Wang DW (2013) Cardiac-specific overexpression of CYP2J2 attenuates diabetic cardiomyopathy in male streptozotocin-induced diabetic mice. *Endocrinology* **154**:2843-2856.

Ma X, Qin X, Shang X, Liu M, and Wang X (2019) Organic anion transport polypeptide 1b2 selectively affects the pharmacokinetic interaction between paclitaxel and

sorafenib in rats. *Biochem Pharmacol* **169**:113612.

Ma X, Shang X, Qin X, Lu J, Liu M, and Wang X (2020) Characterization of organic anion transporting polypeptide 1b2 knockout rats generated by CRISPR/Cas9: A novel model for drug transport and hyperbilirubinemia disease. *Acta Pharm Sin B* **10**:850-860.

Matsumoto S, Hirama T, Kim HJ, Nagata K, and Yamazoe Y (2003) In vitro inhibition of human small intestinal and liver microsomal astemizole O-demethylation: different contribution of CYP2J2 in the small intestine and liver. *Xenobiotica* **33**:615-623.

Matsumoto S, Hirama T, Matsubara T, Nagata K, and Yamazoe Y (2002) Involvement of CYP2J2 on the intestinal first-pass metabolism of antihistamine drug, astemizole. *Drug Metab Dispos* **30**:1240-1245.

Matsumoto S and Yamazoe Y (2001) Involvement of multiple human cytochromes P450 in the liver microsomal metabolism of astemizole and a comparison with terfenadine. *Br J Clin Pharmacol* **51**:133-142.

Mitra R, Guo Z, Milani M, Mesaros C, Rodriguez M, Nguyen J, Luo X, Clarke D, Lamba J, Schuetz E, Donner DB, Puli N, Falck JR, Capdevila J, Gupta K, Blair IA, and Potter DA (2011) CYP3A4 mediates growth of estrogen receptor-positive breast cancer cells in part by inducing nuclear translocation of phospho-Stat3 through biosynthesis of (+/-)-14,15-epoxyeicosatrienoic acid (EET). *J Biol Chem* **286**:17543-17559.

Murray M (2016) CYP2J2 - regulation, function and polymorphism. *Drug Metab Rev*

48:351-368.

Panigrahy D, Kaipainen A, Greene ER, and Huang S (2010) Cytochrome P450-derived eicosanoids: the neglected pathway in cancer. *Cancer Metastasis Rev* **29**:723-735.

Qin X, Lu J, Wang P, Xu P, Liu M, and Wang X (2017) Cytochrome P450 3A selectively affects the pharmacokinetic interaction between erlotinib and docetaxel in rats. *Biochem Pharmacol* **143**:129-139.

Roh J, Rhee J, Chaudhari V, and Rosenzweig A (2016) The Role of Exercise in Cardiac Aging: From Physiology to Molecular Mechanisms. *Circ Res* **118**:279-295.

Saenger AK and Jaffe AS (2007) The use of biomarkers for the evaluation and treatment of patients with acute coronary syndromes. *Med Clin North Am* **91**:657-681

Shao Y, Guan Y, Wang L, Qiu Z, Liu M, Chen Y, Wu L, Li Y, Ma X, Liu M, and Li D (2014) CRISPR/Cas-mediated genome editing in the rat via direct injection of one-cell embryos. *Nat Protoc* **9**:2493-2512.

Wang X, Cheung CM, Lee WY, Or PM, and Yeung JH (2010) Major tanshinones of Danshen (*Salvia miltiorrhiza*) exhibit different modes of inhibition on human CYP1A2, CYP2C9, CYP2E1 and CYP3A4 activities in vitro. *Phytomedicine* **17**:868-875.

Wang X and Yeung JH (2011) Effects of *Salvia miltiorrhiza* extract on the liver CYP3A activity in humans and rats. *Phytother Res* **25**:1653-1659.

Wang X, Tang Y, Lu J, Shao Y, Qin X, Li Y, Wang L, Li D, and Liu M (2016) Characterization of novel cytochrome P450 2E1 knockout rat model generated by CRISPR/Cas9. *Biochem Pharmacol* **105**:80-90.

Xu M, Ju W, Hao H, Wang G, and Li P (2013) Cytochrome P450 2J2: distribution, function, regulation, genetic polymorphisms and clinical significance. *Drug Metab Rev* **45**:311-352.

Zanger UM and Schwab M (2013) Cytochrome P450 enzymes in drug metabolism: regulation of gene expression, enzyme activities, and impact of genetic variation. *Pharmacol Ther* **138**:103-141.

Zhang QY, Raner G, Ding X, Dunbar D, Coon MJ, and Kaminsky LS (1998) Characterization of the cytochrome P450 CYP2J4: expression in rat small intestine and role in retinoic acid biotransformation from retinal. *Arch Biochem Biophys* **353**:257-264.

Zhao Q, Huang J, Wang D, Chen L, Sun D, Zhao C (2018). Endothelium-specific CYP2J2 overexpression improves cardiac dysfunction by promoting angiogenesis via Jagged1/Notch1 signaling. *J Mol Cell Cardiol* **123**:118-127.

Zhou GL, Beloiartsev A, Yu B, Baron DM, Zhou W, Niedra R, Lu N, Tainsh LT, Zapol WM, Seed B, and Bloch KD (2013) Deletion of the murine cytochrome P450 Cyp2j locus by fused BAC-mediated recombination identifies a role for Cyp2j in the pulmonary vascular response to hypoxia. *PLoS Genet* **9**:e1003950.

Footnotes

This work was supported in whole or part by grants from the National Natural Science Foundation of China [81301908, 81773808 and 81830083], and the Science and Technology Commission of Shanghai Municipality [17140901000, 17140901001 and 18430760400]. This work was also supported from ECNU Multifunctional Platform for Innovation [011].

Figure legends

Figure 1. Generation of *CYP2J3/10* knockout rat model. (A) Characterization of precursors for *CYP2J3* (lane 1) and *CYP2J10* (lane 2) sgRNA. (B) Characterization of sgRNA for *CYP2J3* (lane 1) and *CYP2J10* (lane 2). (C) Detection of mutations in the F₀ generation using T7EI assay. T7EI⁻, before T7EI digestion. T7EI⁺, after T7EI digestion. ▶, mutant band. (D) DNA sequencing flanking *CYP2J3* and *CYP2J10* target loci in F₀ rats. “.”, nucleotide deletion. “Δ”, the number of changed nucleotide. “X”, the number of each genotype in four clones.

Figure 2. Off-target analysis of *CYP2J3* (A) and *Cypj10* (B) sgRNA. T7EI⁻, before T7EI digestion; T7EI⁺, after T7EI digestion; OT, off-target site.

Figure 3. The mRNA (A) and protein (B) expression of *CYP2J3*, *CYP2J4* and *CYP2J10* in liver, small intestine and heart of KO rats. The data was expressed as mean ± SD (n=6), and ****p* < 0.001 compared to WT group. N.D., not detected.

Figure 4. Effects of *CYP2J3/10* deletion on the metabolic capacity of CYP2J. (A) Saturation curve of astemizole metabolism in RLM from WT and KO rats. (B) The V_{max} of astemizole metabolism in RLM from WT and KO rats. (C) The Cl_{int} of astemizole metabolism in RLM from WT and KO rats. (D) Pharmacokinetic profiles of astemizole in WT and KO rats. (E) The concentration-time curve of astemizole metabolite (*O*-desmethyl astemizole) in WT and KO rats. The data was expressed as mean ± SD (n=5), and ****p* < 0.001 compared to WT group.

Figure 5. Effects of *CYP2J3/10* deletion on clinical biochemical criterions in rats. (A) Effects on serum protein, alkaline phosphatase, transaminase, bilirubin, triglyceride and

cholesterol. (B) Effects on creatine kinases. All data was expressed as mean \pm SD (n=5), and * p < 0.05, ** p < 0.01 compared to WT group. ALB, albumin; GLB, globulin; TP, total proteins; AP, alkaline phosphatase; AST, aspartate amino transferase; ALT, alanine amino transferase; D-BIL,direct bilirubin; ID-BIL, indirect bilirubin; T-BIL, total bilirubin; TRIG, triglycerides; LDL-CHOL, low-density lipoproteins-cholesterol; HDL-CHOL, high-density lipoproteins-cholesterol; T-CHOL, total cholesterol; CK, creatine kinase.

Figure 6. Compensatory expression of other Cyp isoforms and nuclear receptors in *CYP2J3/10 KO* rats. (A) Compensatory expression in the liver. (B) Compensatory expression in the small intestine. (C) Compensatory expression in the heart. All data was expressed as mean \pm SD (n=5), and * p < 0.05, ** p < 0.01 compared to WT group.

Table 1. Primer pairs used in this study

Primer Name	Primer Sequence (5'→ 3')
<i>CYP2J3</i> -genotyping-F	AACTGGACGGGTATGTAAC
<i>CYP2J3</i> -genotyping-R	ACGCTCTATTGTGGCTTT
<i>CYP2J10</i> -genotyping-F	AAATAGAAGTCAACACCACCAAT
<i>CYP2J10</i> -genotyping-R	ACACGCAGGCAGGAGAAC
<i>CYP2J3</i> -off target-1-F	GACCCTTTCTTTCCAGAC
<i>CYP2J3</i> -off target-1-R	ATGTGACCGCACTTACCC
<i>CYP2J3</i> -off target-2-F	ACTATGGGAGGCAAAGAC
<i>CYP2J3</i> -off target-2-R	TGTGACAGTTACAGGTGGTT
<i>CYP2J3</i> -off target-3-F	GCTGGCTTAAATACACTTGC
<i>CYP2J3</i> -off target-3-R	AATGACTTCCTCCACATCCT
<i>CYP2J3</i> -off target-4-F	TTCTGTCCTCACCCAAAG
<i>CYP2J3</i> -off target-4-R	ACCCTCCTGTAAGCCACT
<i>CYP2J3</i> -off target-5-F	ACAGGCTAGATTCAGACG
<i>CYP2J3</i> -off target-5-R	AGTATTTGCTTTGGTGGG
<i>CYP2J3</i> -off target-6-F	AAAGCCAGTATCCAGAAG
<i>CYP2J3</i> -off target-6-R	GCTATGATGTTCCCAAGT
<i>CYP2J10</i> -off target-1-F	TTCCCAAATCTTTACCAT
<i>CYP2J10</i> -off target-1-R	AGGCTTGTTAATCATCCA
<i>CYP2J10</i> -off target-2-F	TCACTCTGTTTGTGCCTTTA
<i>CYP2J10</i> -off target-2-R	GCAGTATCCTGTCCACCTAT
<i>CYP2J3</i> -Q-PCR-F	CCCTTAGTGGGTTGCTTG
<i>CYP2J3</i> -Q-PCR-R	ACCTCCTTTGCTCCTTCC
<i>CYP2J4</i> -Q-PCR-F	CTGGCCGATCGAGAATCCAT
<i>CYP2J4</i> -Q-PCR-R	TGGTACCCTTTGGCAGGTGG
<i>CYP2J10</i> -Q-PCR-F	CCGGCGTCCCAAGAACTA
<i>CYP2J10</i> -Q-PCR-R	AGGTGTAACAGGGCGATT
<i>β-actin</i> -Q-PCR-F	AGATCAAGATCATTGCTCCTCCT
<i>β-actin</i> -Q-PCR-R	ACGCAGCTCAGTAACAGTCC

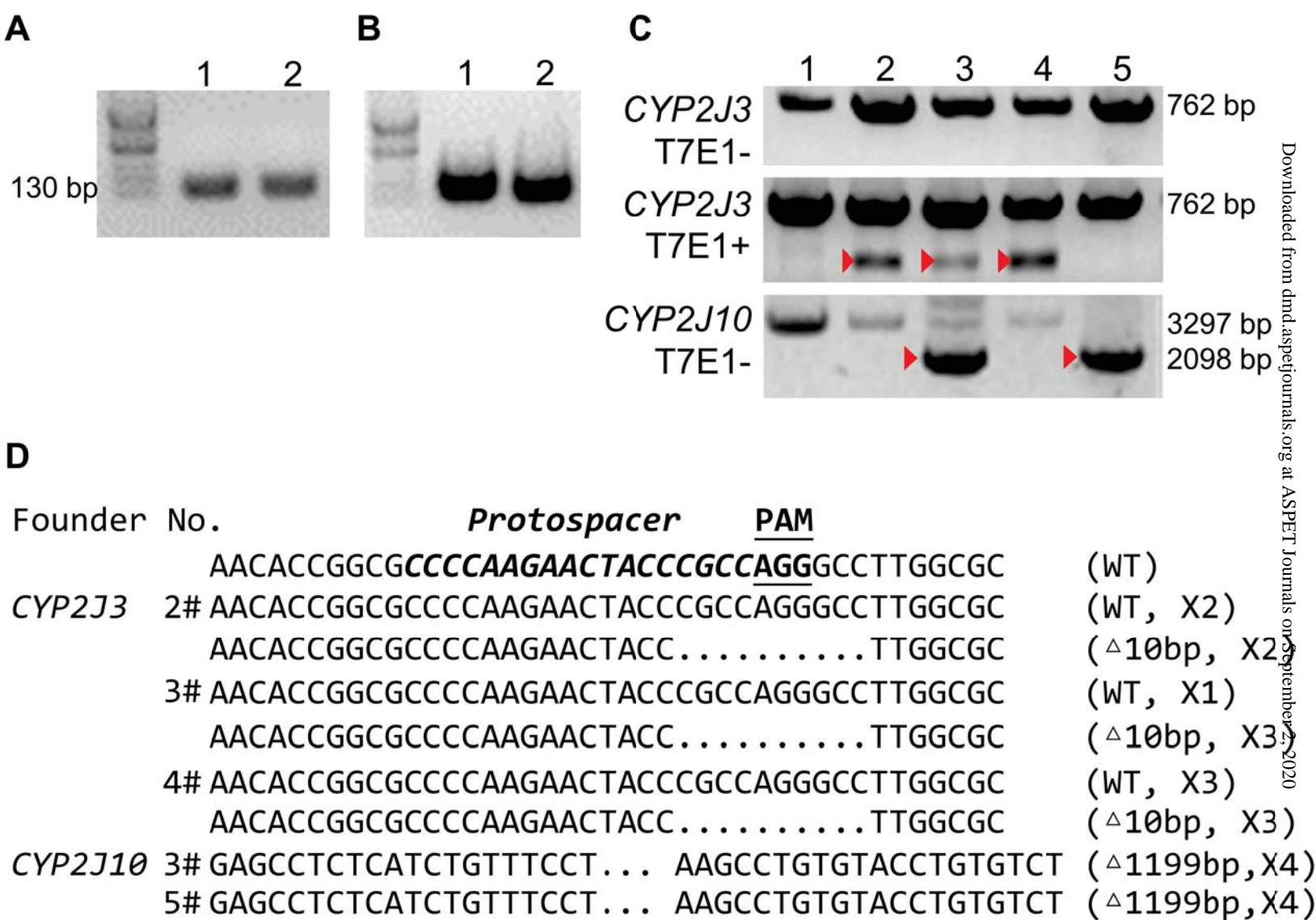
Table 2. Potential off-target sites evaluated through T7E1

Match name	Coordinate	Spacer + <u>PAM</u>	No. of mismatch	Off-target score
<i>CYP2J3</i> sgRNA		CCCCAAGA <u>ACTACCCGCCAGG</u>		
<i>CYP2J3</i> -OT-1	chr11:39820711-39820729	CCAAGgAaTACCCGCC <u>AGG</u>	2	0.35
<i>CYP2J3</i> -OT-2	chr1:89168948-89168964	AAGgACTACCCGCC <u>tGG</u>	2	0.28
<i>CYP2J3</i> -OT-3	chr5:165639577-165639596	CCCCAAGAA <u>tACCCGCCtGG</u>	3	0.25
<i>CYP2J3</i> -OT-4	chr6:125220805-125220824	CCCCAAGAAaA <u>CCCGCCAGG</u>	2	0.25
<i>CYP2J3</i> -OT-5	chr4:144112581-144112600	CCCCAAGAAgaA <u>CCCGCCAGG</u>	2	0.25
<i>CYP2J3</i> -OT-6	chr2:7454206-7454225	CCCCAAGAAgaA <u>CCCGCCAGG</u>	2	0.25
<i>CYP2J10</i> sgRNA		GGTGTAA <u>CAGGGCGATTCAAGG</u>		
<i>CYP2J10</i> -OT-1	chr1:1556325-1556309	TAACAGGGCGATT <u>tGG</u>	1	0.40
<i>CYP2J10</i> -OT-2	chr2:116326415-116326400	AACAGGGCGATT <u>CAAGG</u>	0	0.28

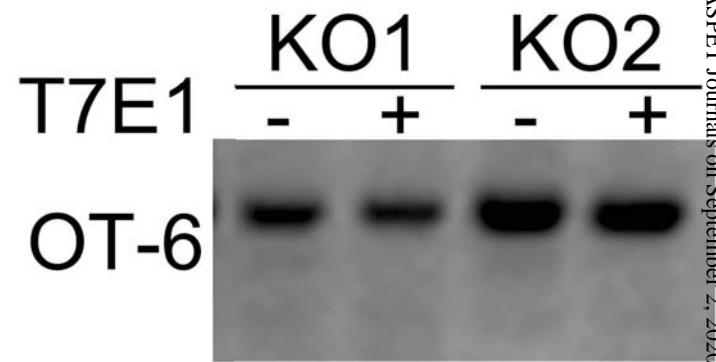
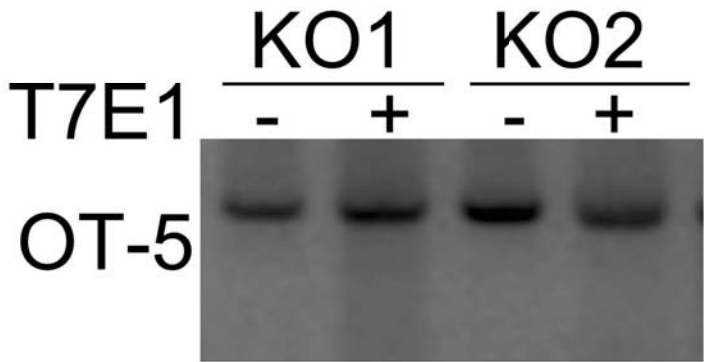
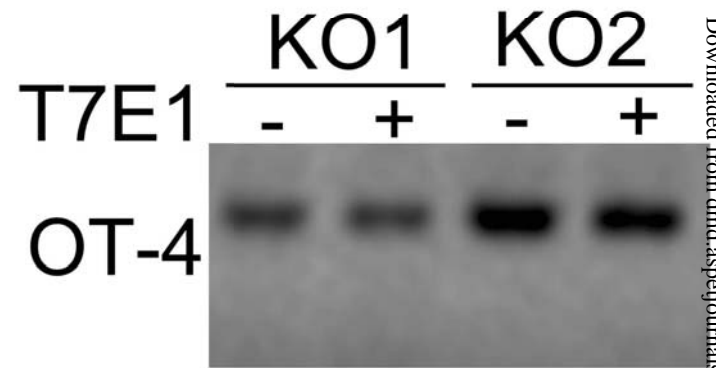
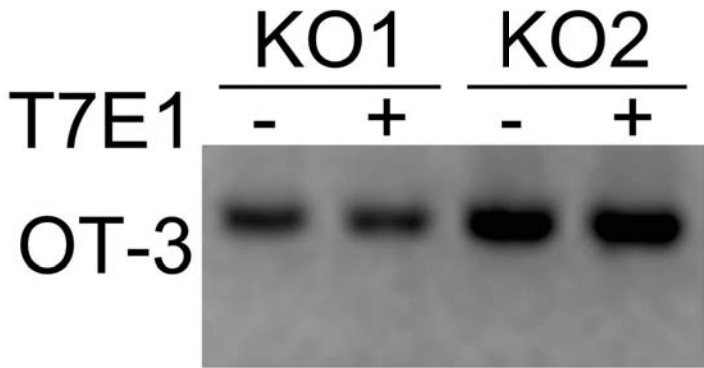
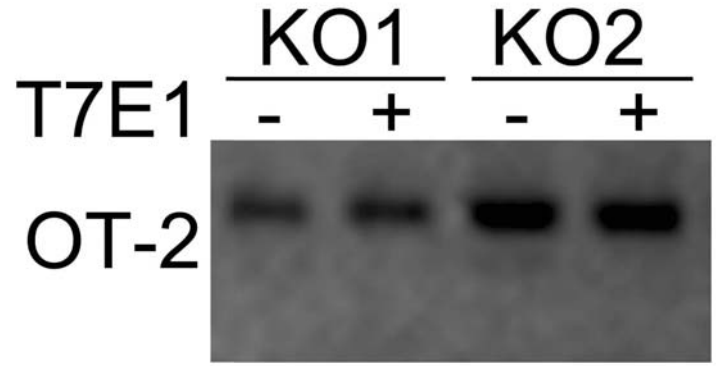
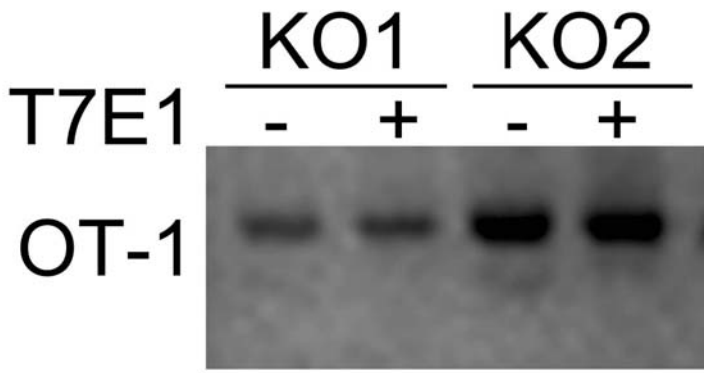
Table 3. Pharmacokinetic parameters of astemizole in WT and KO rats

Parameters	WT	KO
T _{1/2} (min)	170.30 ± 26.89	582.40 ± 155.30 *
T _{max} (min)	57.00 ± 30.89	153.00 ± 27.00 *
C _{max} (ng/mL)	15.37 ± 2.03	36.25 ± 7.60 *
AUC _{0-t} (min*µg/mL)	2.52 ± 0.61	11.50 ± 2.56 **
V _d /F (L/kg)	1705.00 ± 369.30	626.90 ± 124.10 *
CL/F (L/min/kg)	7.63 ± 1.97	0.88 ± 0.23 **
MRT (min)	155.10 ± 12.97	210.70 ± 2.76 **

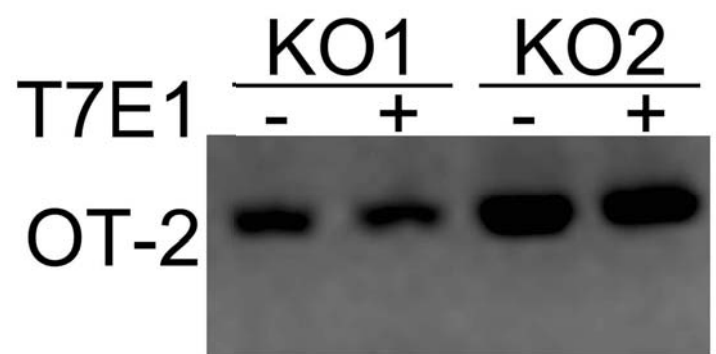
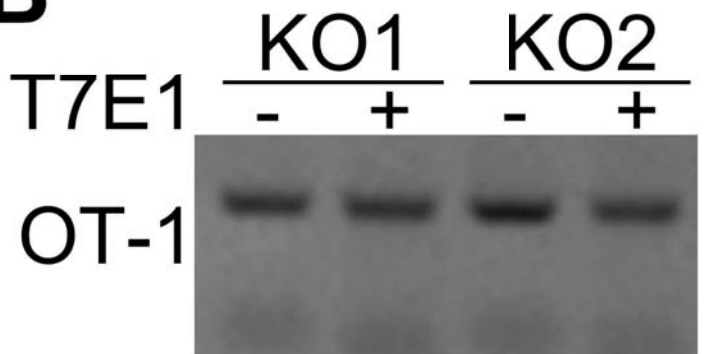
All data was expressed as mean ± SD (n=5), **p*< 0.05 and ***p*< 0.01 compared to WT group.

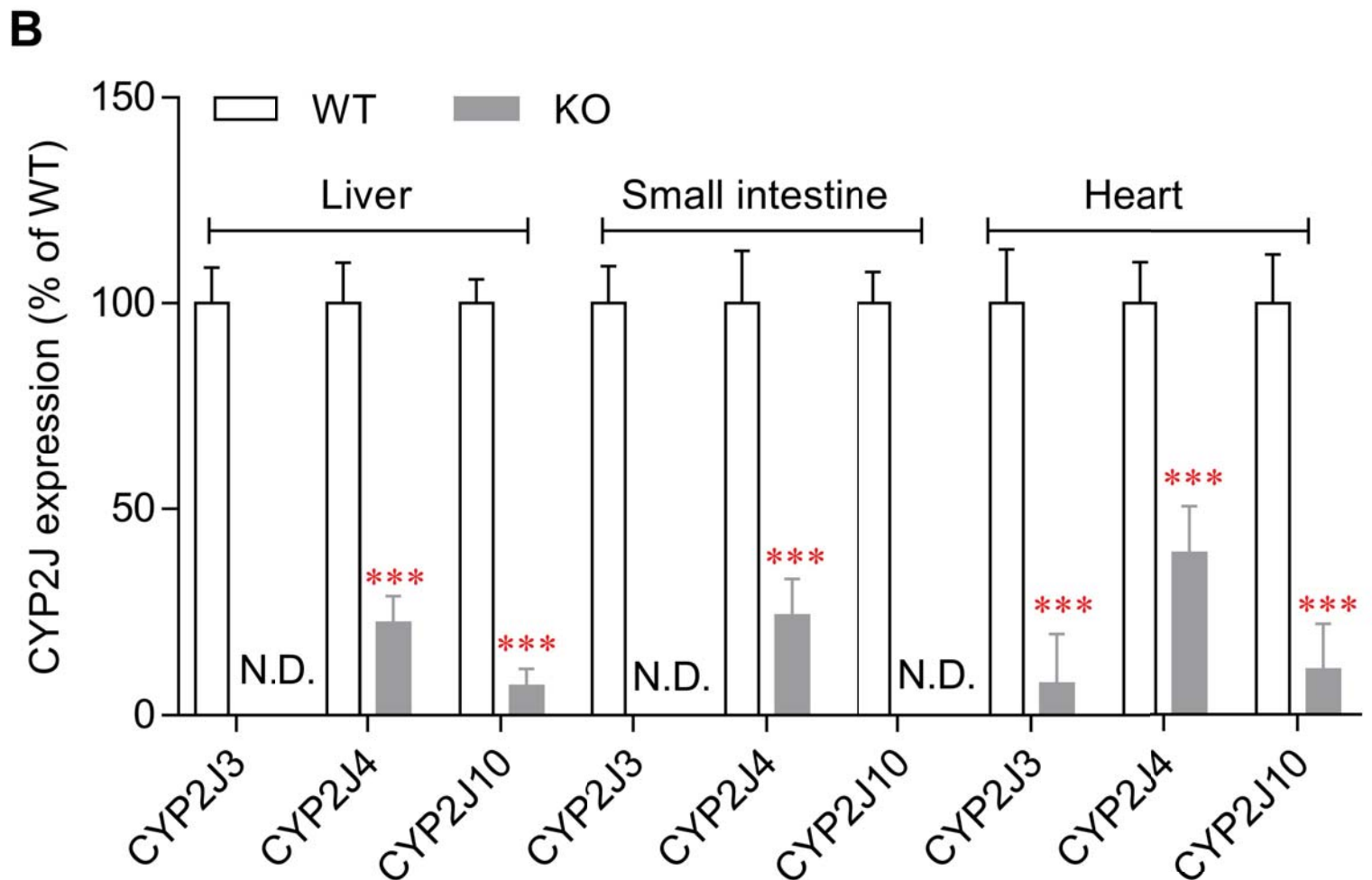
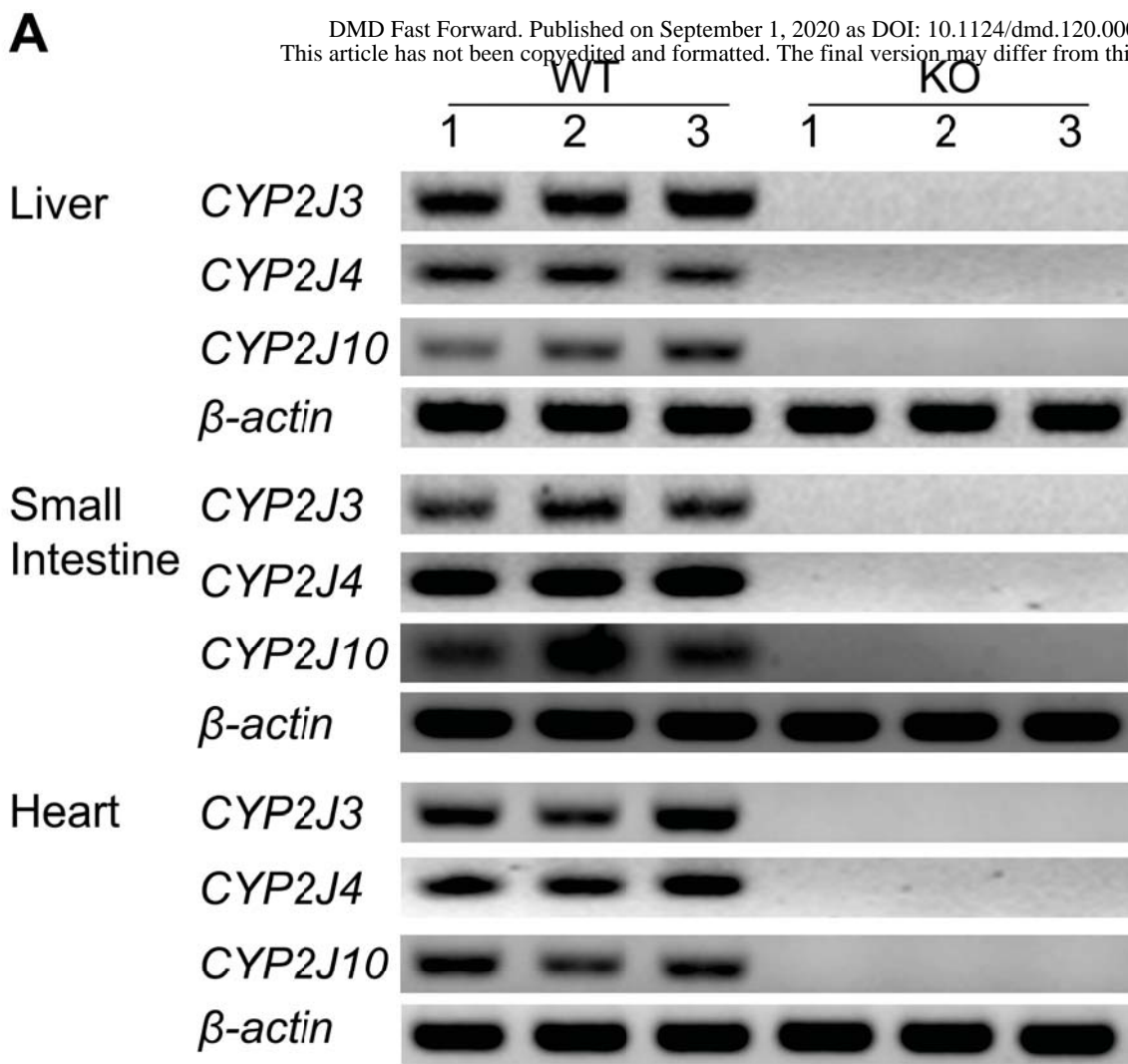


A

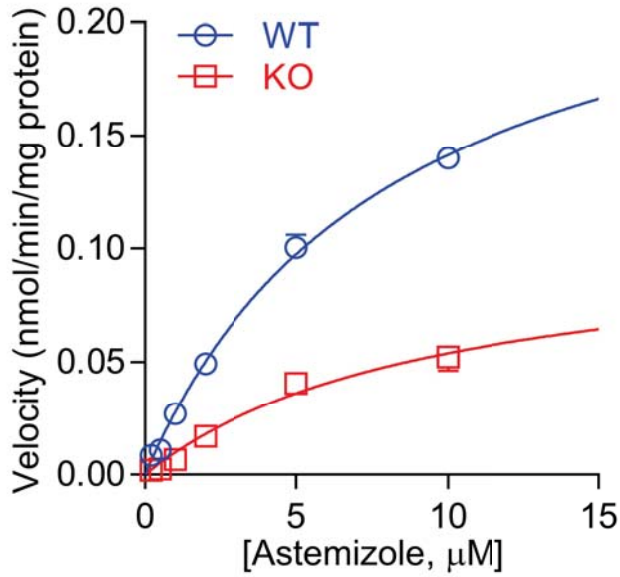


B

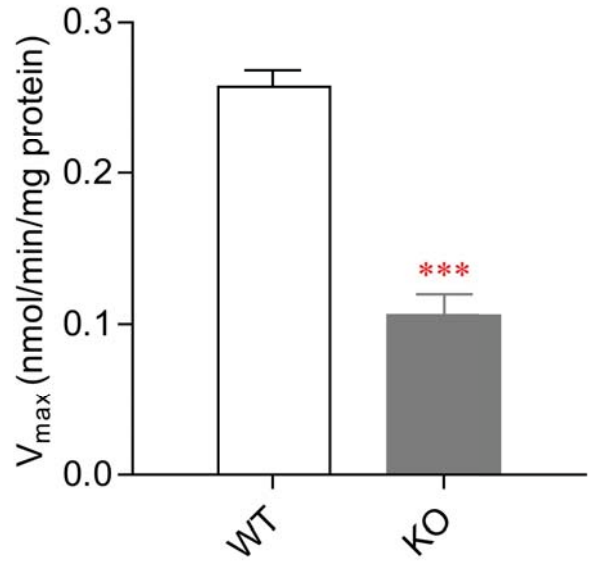




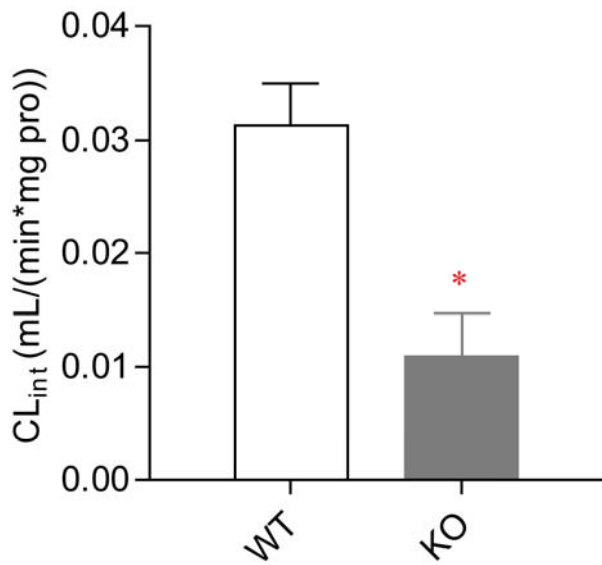
A



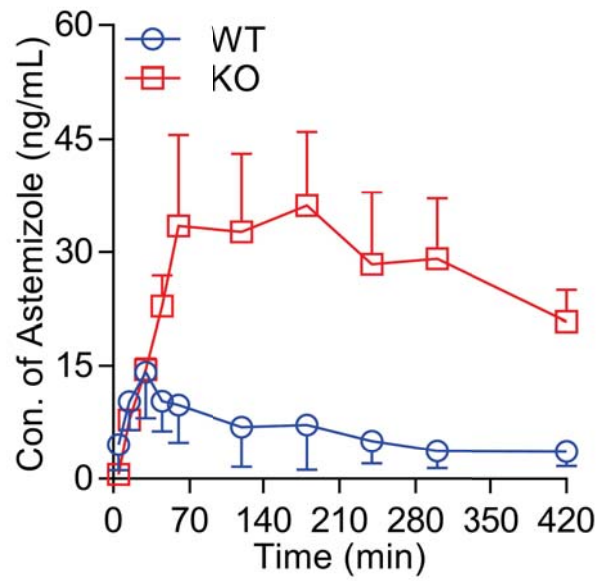
B



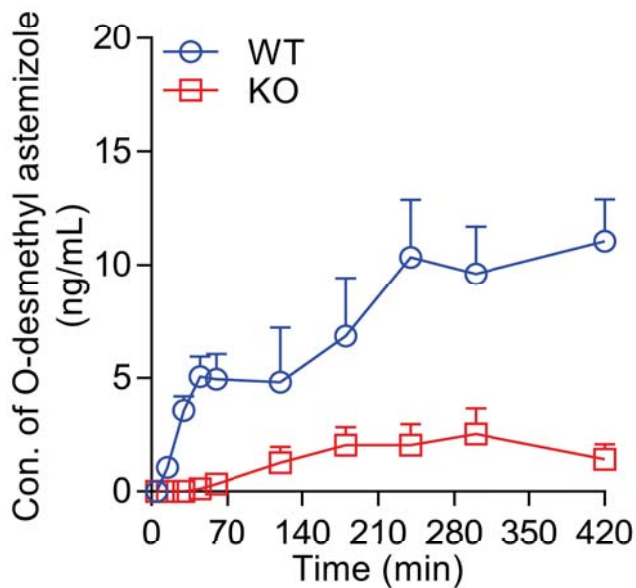
C



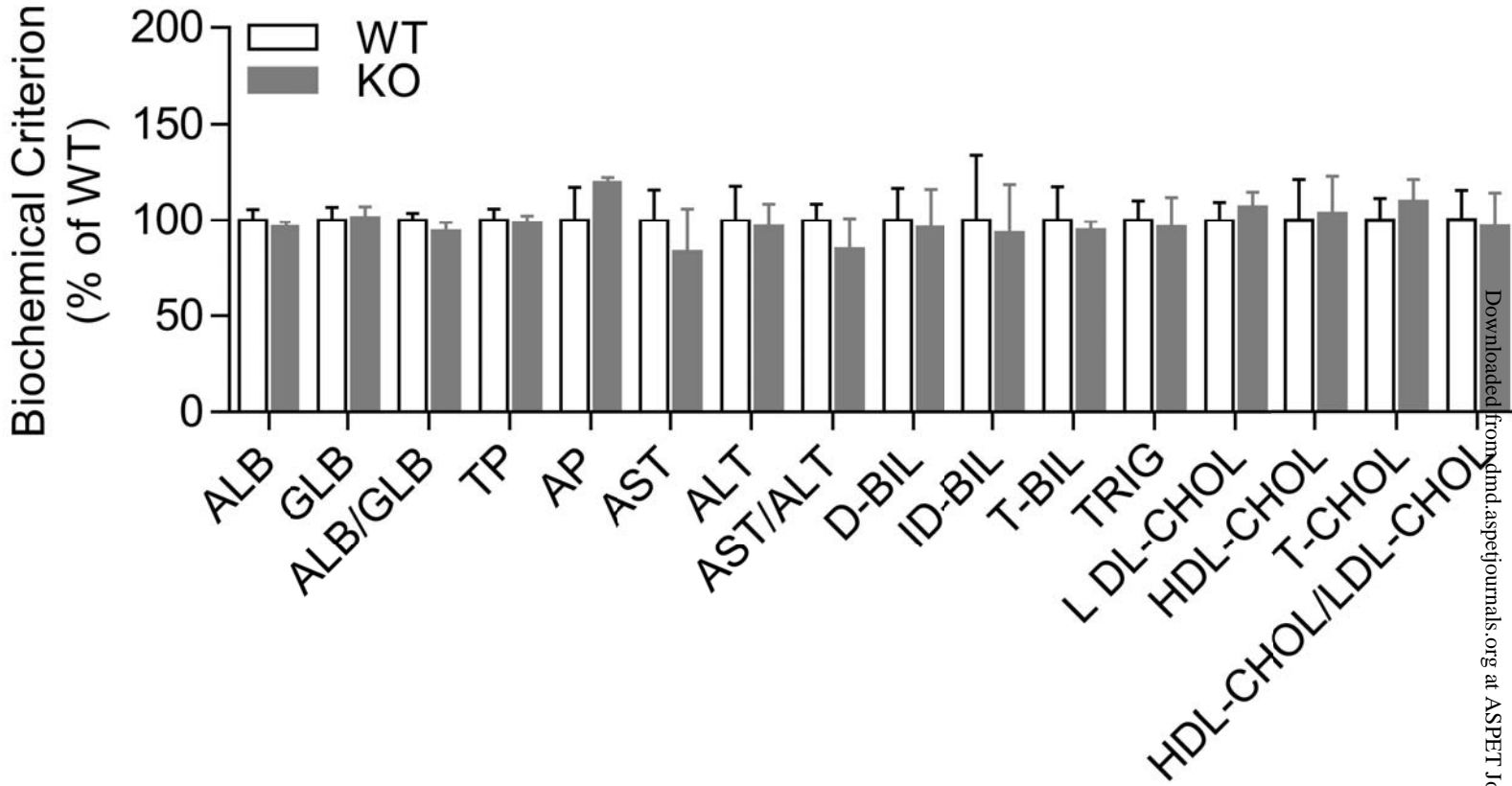
D



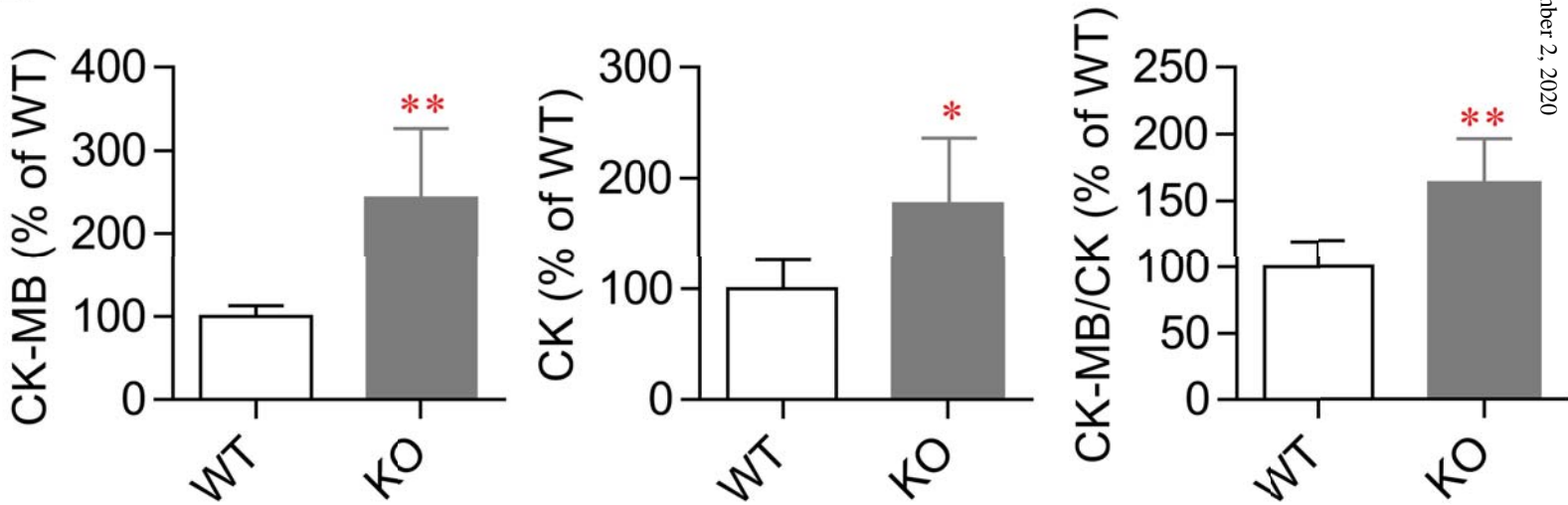
E



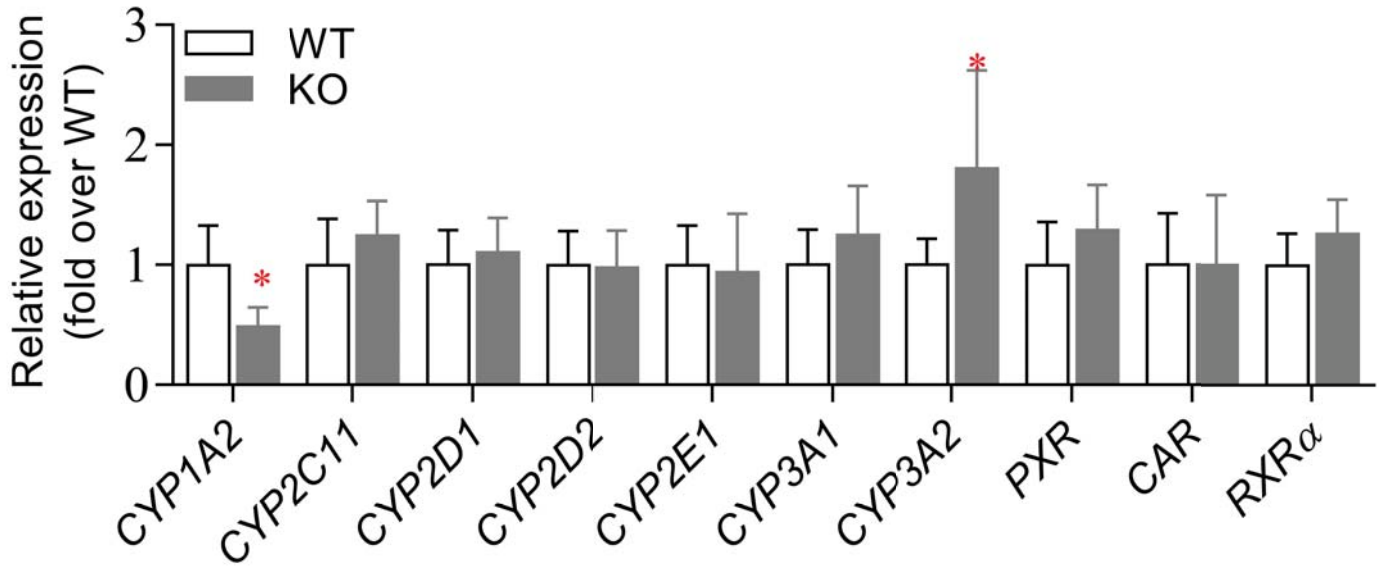
A



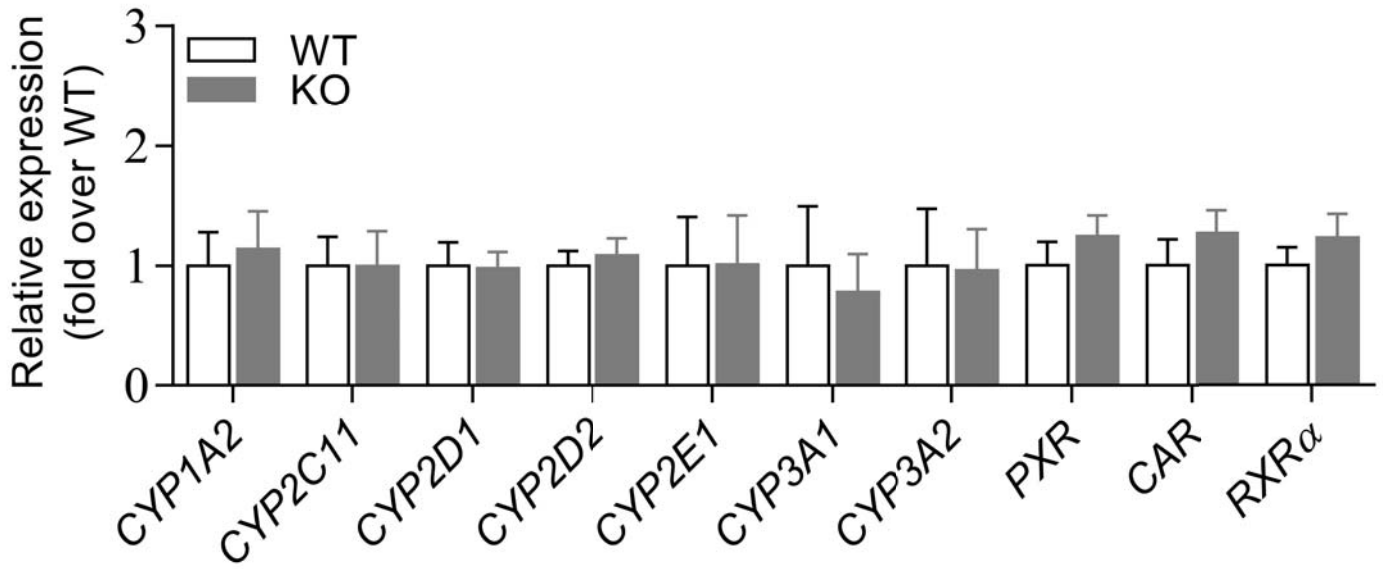
B



A



B



C

